## 5.5 Two-ion anisotropy

In this section, we discuss the components of the two-ion coupling which cannot be included in the *isotropic* Heisenberg Hamiltonian considered hitherto, i.e. the two-ion term in eqn (5.2.1). We first consider the classical magnetic *dipole–dipole interaction* in some detail, and show how it may affect the spin-wave energies and ultrasonic velocities. Thereafter we discuss some of the complexities resulting from the presence of *general two-ion couplings*, which are consistent with the symmetry properties of the magnetic phase. The experimental manifestations of such interactions, which either have been observed in the excitation spectrum of Tb, or could in principle be observed, are finally summarized.

### *5.5.1 The dipole–dipole interaction*

A general two-ion Hamiltonian involving only the dipolar moments of the $4f$ electrons is

$$\mathcal{H}_{\rm dd} = -\frac{1}{2}\sum_{ij}\sum_{\alpha\beta}\mathcal{J}_{\alpha\beta}(ij)J_{i\alpha}J_{j\beta}. \tag{5.5.1}$$

The Heisenberg interaction, when expressed in this way, is diagonal, with the form $\mathcal{J}(ij)\delta_{\alpha\beta}$. The most familiar example of an *anisotropic* two-ion coupling is the classical magnetic dipole–dipole interaction, which gives a contribution

$$\Delta\mathcal{J}_{\alpha\beta}(ij) = \frac{N}{V}(g\mu_B)^2 D_{\alpha\beta}(ij), \tag{5.5.2a}$$

where $D_{\alpha\beta}(ij)$ is the dimensionless coupling parameter

$$D_{\alpha\beta}(ij) = \frac{V}{N}\frac{3(R_{i\alpha}-R_{j\alpha})(R_{i\beta}-R_{j\beta})-\delta_{\alpha\beta}|\mathbf{R}_i-\mathbf{R}_j|^2}{|\mathbf{R}_i-\mathbf{R}_j|^5}, \tag{5.5.2b}$$

recalling that the magnetic moment of the $i$th ion is $g\mu_B\mathbf{J}_i$. This coupling is weak, being typically one or two orders of magnitude smaller than the indirect exchange between near neighbours, but it is extremely long-range and anisotropic and may therefore have important consequences for the magnetic properties, as we shall discuss in the following.

We wish to calculate the spatial Fourier transform

$$D_{\alpha\beta}(\mathbf{q}) = \frac{1}{N}\sum_i\sum_j D_{\alpha\beta}(ij)\, e^{-i\mathbf{q}\cdot(\mathbf{R}_i-\mathbf{R}_j)}. \tag{5.5.3}$$

If $\mathbf{q}$ is along the $c$-axis, which is a three-fold axis of the hcp lattice, the symmetry dictates that the only non-zero elements of $\mathcal{J}_{\alpha\beta}(\mathbf{q})$ are $\mathcal{J}_{\xi\xi}(\mathbf{q}) = \mathcal{J}_{\eta\eta}(\mathbf{q})$ and $\mathcal{J}_{\zeta\zeta}(\mathbf{q})$. In addition, the condition $\sum_\alpha D_{\alpha\alpha}(\mathbf{q}) = 0$ implies that

$$D_{\zeta\zeta}(\mathbf{q}) = -2D_{\xi\xi}(\mathbf{q}) = -2D_{\eta\eta}(\mathbf{q}) \qquad ; \quad \mathbf{q} \parallel c-\text{axis}, \tag{5.5.4}$$

with the extra stipulation that $\mathbf{q} \neq \mathbf{0}$, in which case the surface of the sample does not contribute. In the limit of long wavelengths, the shape of the sample becomes important, and for convenience we assume it to be an ellipsoid, with the principal axes along the symmetry $\xi$-, $\eta$-, and $\zeta$-axes. We consider first the limit $\mathbf{q} = \mathbf{0}$ where, because the sample is an ellipsoid, the summation over $j$ in (5.5.3) leads to a result independent of $i$, since an ellipsoid placed in a constant magnetic field has a uniform magnetization throughout its interior. Furthermore, when $\mathbf{r} = \mathbf{R}_i - \mathbf{R}_j$ becomes large, it may be replaced by a continuous variable, and the sum

over $j$ may be split into a sum over the lattice points lying within a large sphere plus an integral over the rest of the sample:

$$\sum_j \cdots = \sum_{j\in\text{sphere}} \cdots + \frac{N}{V}\int_{\text{sphere}}^{\text{sample}} \cdots d\mathbf{r}.$$

The value of the integral for the $zz$-component is

$$\begin{aligned}\int \frac{1}{r^3}\big(\frac{3z^2}{r^2}-1\big)d\mathbf{r} = -\int \nabla\cdot\Big(\frac{\mathbf{z}}{r^3}\Big)d\mathbf{r} &= \int_{\text{sphere}} \frac{\mathbf{z}\cdot d\mathbf{S}}{r^3} - \int_{\text{sample}} \frac{\mathbf{z}\cdot d\mathbf{S}}{r^3} \\ &= \frac{4\pi}{3} - N_z,\end{aligned}$$

where $d\mathbf{S}$ is a vectorial surface element of the sphere/sample, and $N_\xi$ is the *demagnetization factor*

$$N_\xi = \int_{\text{sample}} \left(\frac{\hat{\boldsymbol{\xi}}\cdot\mathbf{r}}{r^3}\right)\hat{\boldsymbol{\xi}}\cdot d\mathbf{S}, \tag{5.5.5}$$

where $\hat{\boldsymbol{\xi}}$ is a unit vector along the $\xi$-axis. It is easily seen that $N_\xi + N_\eta + N_\zeta = 4\pi$. Hence we obtain

$$D_{\xi\xi}(\mathbf{0}) = \frac{4\pi}{3} + \big[D_{\xi\xi}(\mathbf{0})\big]_L - N_\xi, \tag{5.5.6}$$

plus equivalent results for the other diagonal components. The first term is the *Lorentz factor*, and $\big[D_{\xi\xi}(\mathbf{0})\big]_L$ is the value of the lattice sum over the sphere, satisfying the relations $\big[D_{\zeta\zeta}(\mathbf{0})\big]_L = -2\big[D_{\xi\xi}(\mathbf{0})\big]_L = -2\big[D_{\eta\eta}(\mathbf{0})\big]_L$. In the case of a cubic lattice, the lattice sums vanish by symmetry. This is nearly also true for an hcp lattice with an ideal $c/a$-ratio, because of the close relationship between the fcc lattice and the ideal hcp lattice. The hcp lattice of the heavy rare earths is slightly distorted, as may be seen from Table 1.2, in which case the lattice sums become non-zero, approximately proportionally to the deviation from the ideal $c/a$-ratio; $\big[D_{\xi\xi}(\mathbf{0})\big]_L = -0.0024 + 1.50\big(c/a - \sqrt{8/3}\big)$. Brooks and Goodings (1968) overestimate the anisotropy in the free energy due to the dipole interaction by a factor of two.

When considering the lattice sum determining $D_{\alpha\beta}(\mathbf{q}) - D_{\alpha\beta}(\mathbf{0})$, we may immediately apply the continuum approximation in the long-wavelength limit $2\pi/q \gg a$, and replace the sum with the corresponding integral. In the calculation above at $\mathbf{q} = \mathbf{0}$, this approximation is not directly applicable, because the corresponding integral contains a divergence at the origin, which is however removed in the difference

$D_{\alpha\beta}(\mathbf{q}) - D_{\alpha\beta}(\mathbf{0})$. In addition to the condition $q \ll 2\pi/a$, we shall assume that $q \gg 2\pi/L$, or more specifically $q \geq 10/L$ (Keffer 1966), where $L$ is a length dimension of the crystal, in which case the effects of the boundaries on $D_{\alpha\beta}(\mathbf{q})$ are averaged out because of the relatively rapid variation of the exponential factor on the surface. Using these two conditions, we find

$$\begin{aligned} D_{\alpha\beta}(\mathbf{q}) &= D_{\alpha\beta}(\mathbf{0}) + \int \frac{3(\hat{\boldsymbol{\alpha}}\cdot\mathbf{r})(\hat{\boldsymbol{\beta}}\cdot\mathbf{r}) - \delta_{\alpha\beta}\, r^2}{r^5}\big(e^{i\mathbf{q}\cdot\mathbf{r}} - 1\big)d\mathbf{r} \\ &= \big[D_{\alpha\beta}(\mathbf{0})\big]_L + \\ &\iint \frac{3(\hat{\boldsymbol{\alpha}}\cdot\mathbf{r})(\hat{\boldsymbol{\beta}}\cdot\mathbf{r}) - \delta_{\alpha\beta} r^2}{r^5}\Big[\sum_{l=0}^{\infty}[4\pi(2l+1)]^{1/2}\, i^l\, j_l(qr) Y_{l0}(\theta,\phi)\Big] r^2 dr d\Omega. \end{aligned}$$

The $\mathbf{q}$-independent term in the first integral leads to the same result as in (5.5.6), but without the lattice-sum contribution, and adding $D_{\alpha\beta}(\mathbf{0})$, we are left with the term $\big[D_{\alpha\beta}(\mathbf{0})\big]_L$. The $\mathbf{q}$-dependent exponential is expanded in terms of the spherical Bessel functions, as in (4.1.8), with the polar axis chosen to be parallel to $\mathbf{q}$. The dipole factor in the resulting integral may be written as a linear combination of the spherical harmonics of second rank $Y_{2m}(\theta,\phi)$, multiplied by $r^{-3}$, ensuring that only the term with $l = 2$ in the sum over $l$ survives the integration over solid angles. Further, if $\hat{\boldsymbol{\alpha}}$ and $\hat{\boldsymbol{\beta}}$ are either parallel or perpendicular to $\mathbf{q}$, only the diagonal components may differ from zero. With $\hat{\boldsymbol{\alpha}}$ and $\hat{\boldsymbol{\beta}}$ both parallel to $\mathbf{q}$, the longitudinal component is

$$\begin{aligned} &D_{\parallel}(\mathbf{q}) - \big[D_{\parallel}(\mathbf{0})\big]_L \\ &\quad = \iint [16\pi/5]^{1/2} Y_{20}(\theta,\phi) r^{-3} [4\pi\cdot 5]^{1/2}(-1) j_2(qr) Y_{20}(\theta,\phi) r^2 dr d\Omega \\ &\qquad\qquad = -8\pi \int_0^{\infty} \frac{1}{\rho} j_2(\rho) d\rho = -8\pi\Big[-\frac{j_1(\rho)}{\rho}\Big]_0^{\infty} = -\frac{8\pi}{3}, \end{aligned}$$

recalling that $j_1(\rho)/\rho \to \frac{1}{3}$ or 0, for respectively $\rho \to 0$ or $\infty$. This result implies that the two transverse components are

$$D_{\perp}(\mathbf{q}) - \big[D_{\perp}(\mathbf{0})\big]_L = -\tfrac{1}{2}\big\{D_{\parallel}(\mathbf{q}) - \big[D_{\parallel}(\mathbf{0})\big]_L\big\} = \frac{4\pi}{3}; \qquad (5.5.7)$$
$$\text{when} \quad 2\pi/L \ll q \ll 2\pi/a.$$

The dipole-coupling components change from the values given by (5.5.6) to those above within a very narrow range of $q$, i.e. when $q$ goes from zero to about $10/L$, as shown by the detailed analysis of Keffer (1966). At larger wave-vectors, the variation of $D_{\alpha\beta}(\mathbf{q})$ is smooth and gradual,

and it may be described by a few interplanar coupling parameters of the type used for other two-ion interactions. Cohen and Keffer (1955) have calculated the **q**-dependence for the three cubic Bravais lattices, and their results also determine approximately $D_{\alpha\beta}(\mathbf{q})$, with **q** along the $c$-axis, in the hcp lattice with the ideal $c/a$-ratio, since this is equivalent to **q** along a (111)-direction in the fcc crystal. In the distorted case, with $c/a = 0.963\sqrt{8/3}$ (corresponding to Ho), a numerical calculation gives

$$D_{\xi\xi}(\mathbf{q}) + 0.0221\frac{4\pi}{3} = \left\{0.9190 + 0.0816\cos(qc/2) - 0.0006\cos(qc)\right\}\frac{4\pi}{3}$$

when $\mathbf{q} \parallel c$-axis and $q \geq 10/L$, so that the **q**-dependence in the $c$-direction is very weak, except for the jump at small **q**, which is illustrated for the example of Ho in Fig. 5.7.

In a uniform ferromagnet, the demagnetization factor leads to a positive contribution to the internal energy. Without any external applied

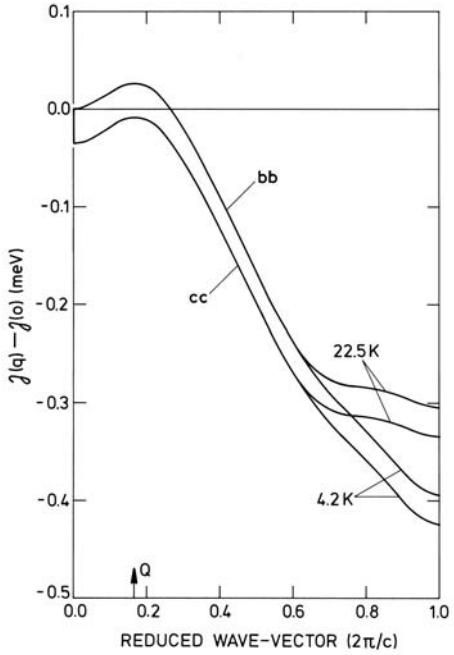


**Fig. 5.7.** Parallel and perpendicular components of the Fourier transform, for **q** along the $c$-direction, of the two-ion coupling in Ho, deduced from the spin-wave energies. The coupling is assumed to comprise an isotropic indirect-exchange contribution and the classical dipole–dipole interaction, which gives rise to the discontinuity at $\mathbf{q} = \mathbf{0}$ in the parallel component, and stabilizes the cone structure at low temperatures.

field, it is therefore energetically favourable for the system to split up in *domains*, in which the magnetization vector points in different directions, so that the magnetization almost vanishes at the surface. The greater the number of domains, the more effectively the demagnetization contribution may be eliminated, but this tendency is opposed by the cost in energy of the *domain-walls*. It is only the contribution due to the demagnetization factor (as determined by the magnetization at the surface) which is affected by the creation of domains, and in a simple model in which the energy of the domain-walls is neglected, the internal energy per unit volume, due to the dipole coupling and including the Zeeman energy, is

$$U_D + U_Z \simeq -\tfrac{1}{2} D_{zz}^{\text{eff}}(\mathbf{0}) M^2 + \tfrac{1}{2} N_z \langle M \rangle^2 - H_A \langle M \rangle.$$

The demagnetization factor is considered separately, so that $D_{zz}^{\text{eff}}(\mathbf{0}) = 4\pi/3 + \big[D_{zz}(\mathbf{0})\big]_L$, and $H_A$ is the field applied in the z-direction. $M$ is the magnetization,

$$M = \frac{N}{V} g \mu_B \langle J_z \rangle \tag{5.5.8}$$

in each domain, whereas $\langle M \rangle$ is the magnetization averaged over the whole crystal. If the *internal field* $H_I$ and the *demagnetization field* $H_D$ are defined by

$$H_I = H_A - H_D \qquad ; \qquad H_D = N_z \langle M \rangle, \tag{5.5.9}$$

the energy is minimized by the conditions; $H_I = 0$ when $\langle M \rangle < M$, and $\langle M \rangle = M$ when $H_I > 0$. As a function of $H_I$, the magnetization jumps from zero to its 'saturation' value at $H_I = 0$.

The strong $\mathbf{q}$-dependence of the dipole coupling at small $\mathbf{q}$ is reflected in the energies of the magnetic excitations. In the case of the anisotropic ferromagnet, it is straightforward to deduce that the two-ion coupling of eqn (5.5.1) leads to spin-wave energies determined by

$$\begin{aligned} E_T^2(\mathbf{q}) = &\big[A_{\mathbf{0}}(T) + B_{\mathbf{0}}(T) + \langle J_z \rangle \{\mathcal{J}_{\xi\xi}(\mathbf{0}) - \mathcal{J}_{\zeta\zeta}(\mathbf{q})\}\big] \\ &\times \big[A_{\mathbf{0}}(T) - B_{\mathbf{0}}(T) + \langle J_z \rangle \{\mathcal{J}_{\xi\xi}(\mathbf{0}) - \mathcal{J}_{\eta\eta}(\mathbf{q})\}\big] - \big[\langle J_z \rangle \mathcal{J}_{\eta\zeta}(\mathbf{q})\big]^2, \end{aligned} \tag{5.5.10}$$

assuming that the magnetization vector in the basal plane is parallel to the $\xi$-axis, and that $\mathcal{J}_{\eta\zeta}(\mathbf{q}) = \mathcal{J}_{\zeta\eta}(\mathbf{q})$. This result may be obtained by an extension of the procedure used in Section 5.2, most easily from the MF susceptibility (5.2.42). Introducing the above results into this expression, we find, at $\mathbf{q} \equiv \mathbf{0}$,

$$E_T^2(\mathbf{0}) = \big[A'_{\mathbf{0}}(T) + B'_{\mathbf{0}}(T) + g\mu_B \langle M \rangle N_\zeta\big]\big[A_{\mathbf{0}}(T) - B_{\mathbf{0}}(T) + g\mu_B \langle M \rangle N_\eta\big], \tag{5.5.11a}$$

where the $H$ appearing in $A_{\mathbf{0}}(T)$ in (5.2.37) or (5.3.22) is the internal field $H_I$, and

$$A'_{\mathbf{0}}(T) + B'_{\mathbf{0}}(T) = A_{\mathbf{0}}(T) + B_{\mathbf{0}}(T) + g\mu_B M\big(\big[D_{\xi\xi}(\mathbf{0})\big]_L - \big[D_{\zeta\zeta}(\mathbf{0})\big]_L\big). \tag{5.5.11b}$$

In comparison with the other anisotropy terms, the lattice-sum contribution to $A'_{\mathbf{0}}(T)+B'_{\mathbf{0}}(T)$ is very small (except in Gd) and may be neglected. Equation (5.5.11) demonstrates that the energy gap at $\mathbf{q} = \mathbf{0}$ depends on the shape of the sample, as was first pointed out by Kittel (1948). The same is the case with all other spin-wave modes in the *magnetostatic region* $q \leq 10/L$, which are the observable states in ferromagnetic resonance experiments. In a neutron-scattering experiment, the volume in reciprocal space enclosed by the resolution function is normally several orders of magnitude larger than the volume of the magnetostatic region. The spin-waves in the long-wavelength limit, detected by inelastic neutron-scattering, therefore emanate from the much larger region where $q \geq 10/L$, but is still much smaller than $2\pi/a$, so that any two-ion coupling, except for the dipole coupling, is the same as that at $\mathbf{q} = \mathbf{0}$. The spin-wave energies in this regime are determined by eqn (5.5.10), when the dipole-coupling tensor in (5.5.7) is transformed to the $(\xi\eta\zeta)$-coordinate system, and are

$$\begin{aligned} E_T^2(\mathbf{q} \approx \mathbf{0}) = E_T^2(\widetilde{\mathbf{0}}) + 4\pi g\mu_B M\big[\{A_{\mathbf{0}}(T) - B_{\mathbf{0}}(T)\}\cos^2\theta_{\mathbf{q}} \\ + \{A'_{\mathbf{0}}(T) + B'_{\mathbf{0}}(T)\}\sin^2\theta_{\mathbf{q}}\sin^2\phi_{\mathbf{q}}\big], \end{aligned} \tag{5.5.12a}$$

where $(\theta_{\mathbf{q}}, \phi_{\mathbf{q}})$ are the polar angles of $\mathbf{q}$ with respect to the $c$-axis or $\zeta$-axis, and

$$E_T^2(\widetilde{\mathbf{0}}) = \big[A'_{\mathbf{0}}(T) + B'_{\mathbf{0}}(T)\big]\big[A_{\mathbf{0}}(T) - B_{\mathbf{0}}(T)\big]. \tag{5.5.12b}$$

As long as the magnetization is in the basal-plane, this result is generally valid if $\phi_{\mathbf{q}}$ is redefined to be the angle between the magnetization vector and the projection of $\mathbf{q}$ on the basal-plane. $E_T(\widetilde{\mathbf{0}})$ is the minimum excitation energy, and the corresponding spin waves propagate parallel to the magnetization vector. If $A'_{\mathbf{0}}(T) + B'_{\mathbf{0}}(T)$ is significantly larger than $A_{\mathbf{0}}(T) - B_{\mathbf{0}}(T)$ (in Tb it is an order of magnitude greater at $T = 0$), the maximum value of $E_T(\mathbf{q} \approx \mathbf{0})$ occurs when $\mathbf{q}$ lies in the basal plane perpendicular to the magnetic moments, whereas the spin waves propagating in the $c$-direction only have an energy slightly greater than $E_T(\widetilde{\mathbf{0}})$. An inelastic neutron-scattering experiment, with the mean value of the scattering vector equal to a reciprocal lattice vector, will sample a whole spectrum of spin waves with energies between the two extremes. The shape of the scattering peak will be dependent on the

form of the resolution function. With a spherical resolution, the scattering will be quite sharply peaked at the intermediate energy of the spin waves propagating in the $c$-direction, as illustrated in the case of Tb in Fig. 5.8. The calculated sharp peak at about 1.8 meV and the high-energy shoulder are clearly apparent in the experimental measurements of Houmann *et al.* (1975a). In the measurements of Bjerrum Møller and Mackintosh (1979), on the other hand, the resolution function was such that the modes propagating in the basal plane perpendicular to the magnetization were most heavily weighted, so that the predominant peak occurs at about 2.0 meV. In Ho, the effect of the dipole interaction on the long-wavelength spin waves is even more pronounced. This is an example of the opposite extreme, where $A'_{\mathbf{0}}(T) + B'_{\mathbf{0}}(T)$ is much smaller than $A_{\mathbf{0}}(T) - B_{\mathbf{0}}(T)$, so that the maximum value of $E_T(\mathbf{q} \approx \mathbf{0})$ occurs when $\mathbf{q}$ lies along the $c$-direction. As illustrated in Fig. 5.9, the dipolar splitting in this case is sufficiently great that the neutron scattering at $\mathbf{q} \approx \mathbf{0}$ can be resolved into two peaks.

Another consequence of the strong directional dependence of the dipolar contributions to the spin-wave energies is found in the behaviour of the coupled magneto-acoustic sound waves, discussed in the previous section. The region in $\mathbf{q}$-space sampled in ultrasonic measurements (with frequencies in the MHz regime) is just that in which eqn (5.5.12)

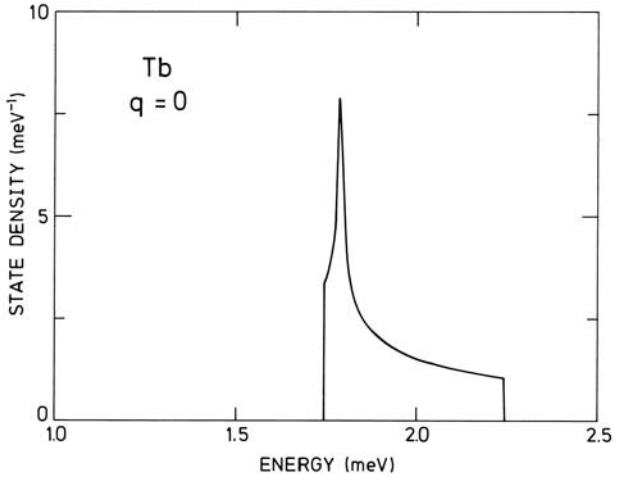


**Fig. 5.8.** The state density of the long-wavelength spin-wave mode $E_T(\mathbf{q} \approx \mathbf{0})$ in Tb at 4 K, calculated from eqn (5.5.12), taking into account the splitting of the dispersion relations by the dipole–dipole interaction. The sharp peak is due to the branch in the $c$-direction.

applies. If **q** is parallel to the magnetization, the spin-wave energies are unchanged from the values deduced in Sections 5.2–4, provided that the lattice-sum contribution is included in the axial anisotropy term (5.5.11*b*), and eqn (5.4.38) is still valid. On the other hand, when **q** is in the basal-plane and perpendicular to the magnetization, the ultrasonic

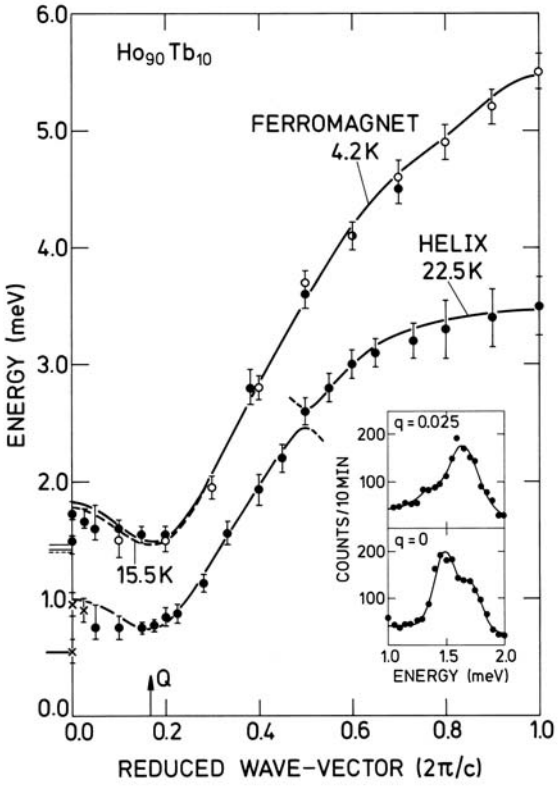


**Fig. 5.9.** Dispersion relations, in the double-zone representation, for magnetic excitations propagating in the *c*-direction of $Ho_{90}Tb_{10}$ in the ferromagnetic phase (upper branch), and the bunched helical structure (lower branch). The full and dashed lines for the ferromagnetic phase show the theoretical dispersion relations at 4 K and 16 K respectively, and the open and filled symbols are the corresponding experimental results. The calculated long-wavelength energies in the basal plane are shown to the left of the ordinate axis and the discontinuity, which is due to the dipole–dipole interaction, is clearly manifested in the neutron-scattering spectra in the inset. This discontinuity also appears in the helical phase, and the bunching causes an energy gap on the ALH face of the Brillouin zone, which is not resolved in these measurements.

velocities are determined by

$$\frac{c^*_{cc}}{c_{66}} = 1 - \frac{\Lambda_\gamma}{A_{\mathbf{0}}(T) - B_{\mathbf{0}}(T) + 4\pi g\mu_B M} \qquad ; \quad \mathbf{q} \perp \langle \mathbf{J} \rangle. \tag{5.5.13}$$

This modification means that only the velocity of those magneto-acoustic modes which propagate parallel to the magnetization vanishes at the critical field $H_I = H_c$ where, according to (5.4.15), $A_{\mathbf{0}}(T) - B_{\mathbf{0}}(T) = \Lambda_\gamma$, whereas the velocity of the modes propagating in the basal-plane perpendicular to the field remains non-zero. This difference in the velocities of the ultrasonic modes was very clearly manifested in the ultrasonic experiment on Tb discussed in Section 5.4 (Jensen and Palmer 1979). This example shows that the dipolar coupling is able to lift the degeneracy in the velocities of two transverse sound-waves which are related to each other by an interchange of the directions of the wave-vector and the polarization vector. The same effect may be produced by the torque exerted on the moments when the local magnetic anisotropy axes are rotated by the transverse phonons relative to the direction of an external magnetic field. As discussed by Melcher (1972) and Dohm and Fulde (1975) the influence of this mechanism on the sound velocities may be derived from the principle that the total system has to be *rotationally invariant*. Their theory has been extended by Jensen (1988b), who finds that the dipolar-coupling contribution strongly dominates in a ferromagnet, but that the importance of the two mechanisms may be comparable in paramagnets.

### *5.5.2 General two-ion interactions*

The two-ion couplings described by eqn (5.5.1) only involve the dipolar moments of the $4f$ electrons. A more general two-ion Hamiltonian is

$$\mathcal{H}_{\mathrm{JJ}} = -\frac{1}{2}\sum_{ij}\sum_{l+l':\mathrm{even}}\sum_{mm'}\big[K^{mm'}_{ll'}(ij)\widetilde{O}_{lm}(\mathbf{J}_i)\widetilde{O}_{l'm'}(\mathbf{J}_j) + (-1)^{m+m'}\{K^{mm'}_{ll'}(ij)\}^*\widetilde{O}_{l\,-m}(\mathbf{J}_i)\widetilde{O}_{l'\,-m'}(\mathbf{J}_j)\big], \tag{5.5.14}$$

expressed in terms of the *Racah operators* or *tensor operators* $\widetilde{O}_{lm}(\mathbf{J}_i)$ introduced in Section 1.4, rather than the Stevens operators. Tables of these operators and a discussion of their properties may be found in Buckmaster *et al.* (1972) and in Lindgård and Danielsen (1974). Here we neglect the possible effects of the *polar* tensors, which vanish for the isolated ions. In principle, these polar tensors may be non-zero in the hcp metals, because the surroundings lack inversion symmetry, but they occur only because of odd-parity configuration-mixing of the $4f$ wavefunctions, which should be insignificant for the ground-state multiplet.

This leaves only the *axial* tensors, i.e. magnetic multipoles of odd rank and electric multipoles of even rank. Time reversal of these tensors effects the transformation $c\widetilde{O}_{lm} \rightarrow c^*(-1)^{l+m}\widetilde{O}_{l\,-m}$, whereas Hermitian conjugation gives $\left(c\widetilde{O}_{lm}\right)^\dagger = c^*(-1)^m\widetilde{O}_{l\,-m}$. The requirement that $\mathcal{H}_{\rm JJ}$ should be invariant under both transformations allows only those terms in eqn (5.5.14) for which $l + l'$ is even. The violation of time-reversal symmetry which occurs when the system is magnetically ordered implies that $\mathcal{H}_{\rm JJ}$ should be supplemented by interactions proportional to $\langle\widetilde{O}_{\lambda\mu}\rangle\widetilde{O}_{lm}(\mathbf{J}_i)\widetilde{O}_{l'm'}(\mathbf{J}_j)$, satisfying the condition that $\lambda + l + l'$ is even. An obvious example is magnetoelastic contributions to the Hamiltonian such as eqn (5.4.5). The tensor operators in (5.5.14) emanate from localized $4f$ wavefunctions with the orbital quantum number $l_{\rm f} = 3$, which puts the further restriction on the phenomenological expansion of $\mathcal{H}_{\rm JJ}$ that $l$ and $l'$ cannot be larger than $2l_{\rm f}+1 = 7$, as the operator-equivalents of higher rank than this vanish identically.

In the rare earth metals, several different mechanisms may give rise to such anisotropic two-ion couplings, and these have been listed by, for instance, Wolf (1971) and Jensen *et al.* (1975). We have already considered the magnetostatic coupling of lowest rank in the magnetic multipole expansion, namely the classical magnetic dipole–dipole interaction. This is of importance only because of its long range. The higher order magnetostatic couplings are of shorter range ($\propto (1/r)^{l+l'+1}$) and have negligible effects. The electrostatic Coulomb interaction gives rise to terms in (5.5.14) in which both $l$ and $l'$ are even. The single-ion contributions ($l' = 0$) are of decisive importance, when $L \neq 0$, but even the lowest-order electrostatic two-ion term, which contributes to the quadrupole–quadrupole interactions, is so small that it may be neglected.

The overlap between the $4f$ wavefunctions of neighbouring ions is so weak that it cannot generate any two-ion coupling of significance. The dominant terms in the two-ion Hamiltonian $\mathcal{H}_{\rm JJ}$ therefore arise indirectly via the propagation of the conduction electrons. We have already mentioned in Section 1.4 the most important of these, due to the exchange interaction between the band electrons and the $4f$ electrons, and it will be discussed in more detail in Section 5.7. In the simplest approximation, the indirect exchange is invariant with respect to a uniform rotation of the angular momenta, i.e. this RKKY interaction is *isotropic*. However, the neglect of the contribution of the orbital moment in the scattering process is not generally justified. If $L$ is non-zero, the orbital state of the $4f$ electrons may change in an exchange-scattering process, if the conduction electron is scattered into a state with a different orbital momentum relative to the ion. The leading-order corrections to the isotropic RKKY interaction due to such processes have been

considered by Kaplan and Lyons (1963) and Kasuya and Lyons (1966). In order to obtain an estimate of the importance of the corrections, they assumed plane-wave states for the conduction electrons, expanded in a series of spherical Bessel functions centred at the ion. These calculations indicated anisotropic two-ion couplings with a magnitude of the order of 10% of the isotropic coupling, or greater (Specht 1967). As discussed in Section 1.3, the free-electron model does not provide a very satisfactory description of the conduction electrons in the rare earths. It is particularly inadequate when orbital effects are involved, since the expansion of the plane-wave states clearly underestimates the $(l = 2)$-character of the $d$-like band-electrons, which dominates the exchange interaction in the $(L = 0)$-case of Gd (Lindgård *et al.* 1975). When $L$ is non-zero, the *Kaplan–Lyons* terms may be of comparable importance to the RKKY interaction in the rare earth metals. The relativistic modification of the band states, due to the spin–orbit coupling, may enhance the orbital effects and also lead to anisotropic interactions in Gd. In addition to the exchange, the direct Coulomb interaction between the $4f$ and the band electrons may contribute to eqn (5.5.14), with terms in which $l$ and $l'$ are both even. This coupling mechanism, via the conduction electrons, is probably more important for this kind of term than the direct electrostatic contribution mentioned above.

The RKKY interaction is derived on the assumption that the $4f$ electrons are localized in the core, and that their mixing with the conduction electrons is exclusively due to the exchange. However, the Coulomb interaction may lead to a slight hybridization of the localized $4f$ states with the band states. In recent years, Cooper and his co-workers (Cooper *et al.* 1985; Wills and Cooper 1987) have analysed the consequences of a weak hybridization between an ion with one or two $f$ electrons and the band electrons, with special reference to the magnetic behaviour of Ce compounds and the actinides. They find that the magnetic two-ion coupling becomes highly anisotropic in the Ce compounds. Although Ce is the rare earth element in which the strongest hybridization effects would be expected to occur, these results and the analysis of Kaplan and Lyons (1963) suggest that the presence of anisotropic two-ion couplings should be a common feature in rare earth metals with orbital angular momentum on the ion.

As is clear from the above discussion, an analysis from first principles cannot at present give a reliable estimate of the relative magnitude of the Heisenberg exchange interaction and the various possible anisotropic two-ion couplings in the rare earth metals. We cannot a priori exclude any terms of the form given by eqn (5.5.14). In order to arrive at such an estimate, it is necessary to calculate the consequences of the anisotropic two-ion terms and compare the predictions with exper-

imental observations. In the case of the nearly saturated ferromagnet, it is straightforward to take into account the effects of $\mathcal{H}_{\rm JJ}$ on the ground-state properties and the spin-waves. The Racah operators, defined with reference to the $(\xi, \eta, \zeta)$-coordinate system, may be expanded in terms of the spin deviation operators. When the moments in the basal-plane ($\theta = \pi/2$) are close to their saturation value ($\langle J_z \rangle \simeq J$),

$$\langle \widetilde{O}_{lm} \rangle \simeq \left( \frac{4\pi}{2l+1} \right)^{1/2} J^{(l)} Y_{lm}(\theta = \frac{\pi}{2}, \phi) = J^{(l)} \Gamma_{lm}\, e^{im\phi}, \qquad (5.5.15a)$$

where

$$\Gamma_{lm} = \begin{cases} (-1)^{(l+m)/2} \dfrac{[(l+m)!(l-m)!]^{1/2}}{(l+m)!!(l-m)!!} & , \; l+m \text{ even} \\ 0 \qquad , \qquad l+m \text{ odd.} \end{cases} \qquad (5.5.15b)$$

Utilizing the equivalence between the Racah operators and the spherical harmonics, and the connection between the spin-wave energies and the angular derivatives of the expectation values (which leads to the relation (5.3.14)), we have to first order in $1/J$ (Jensen *et al.* 1975):

$$\widetilde{O}_{lm}(\mathbf{J}_i) = \Big(1 - \frac{m}{\sqrt{2J}}(a_i^+ - a_i) - \frac{l(l+1)}{2J} a_i^+ a_i - \frac{l(l+1) - 2m^2}{4J}(a_i^+ a_i^+ + a_i a_i)\Big) \times J^{(l)} \Gamma_{lm} e^{im\phi}, \qquad (5.5.16a)$$

if $l+m$ is even, and if $l+m$ is odd

$$\widetilde{O}_{lm}(\mathbf{J}_i) = \big[(l+1)^2 - m^2\big]^{1/2} \Big( \frac{1}{\sqrt{2J}}(a_i^+ + a_i) - \frac{m}{2J}(a_i^+ a_i^+ - a_i a_i) \Big) J^{(l)} \Gamma_{l+1\, m} e^{im\phi}. \qquad (5.5.16b)$$

Introducing these expressions into the two-ion Hamiltonian, we may derive the spin-wave energies, to leading order in $1/J$. The number of terms in eqn (5.5.14) which contribute to the excitation energies, in this order, may be reduced by the symmetry elements of the lattice which leave the **q**-vector unchanged. In the simplest case, where **q** is along the $c$-axis, the three-fold symmetry about this axis plus the mirror-plane perpendicular to the $\xi$-axis (i.e. the $a$-axis) ensure that only terms with $m + m' = 3p$, where $p$ is an integer, contribute, and that their contribution is proportional to $\cos(3p\phi)$. The terms in which $p$ is an odd integer couple the acoustic and optical magnons, but they do not

lift the degeneracy of the modes at A on the Brillouin-zone boundary of Fig 1.4. When $\mathbf{q}$ is parallel to the $c$-axis, a direct calculation of the spin-wave energies (Jensen *et al.* 1975) shows that the two-ion terms in $\mathcal{H}_{\rm JJ}$ lead to the following modifications of the earlier results (5.2.38) and (5.3.22):

(i) The two-ion anisotropy may contribute to the parameters $A_{\mathbf{q}}(T) \pm B_{\mathbf{q}}(T)$ at zero wave-vector.
(ii) $B_{\mathbf{q}}(T)$ becomes dependent on $\mathbf{q}$ to leading order in $1/J$.
(iii) The $\mathbf{q}$-dependent parts of $A_{\mathbf{q}}(T) \pm B_{\mathbf{q}}(T)$ may change when the direction of magnetization is changed.

There are no direct ways of separating the single- and two-ion contributions to the energy gap at zero wave-vector. However, a strong $\mathbf{q}$-dependence of $B_{\mathbf{q}}(T)$ is only possible if the two-ion Hamiltonian is anisotropic. One way to determine $B_{\mathbf{q}}(T)$ is to utilize the dependence of the neutron cross-section on this parameter, given by eqn (5.2.41). This method requires accurate intensity measurements and is not straightforward. The other possibility is to measure the field dependence of the spin-wave energies since, from (5.2.38) or (5.3.22),

$$\alpha_{\mathbf{q}}(T) \equiv \partial E_{\mathbf{q}}^2(T)/\partial(g\mu_B H) \simeq 2A_{\mathbf{q}}(T), \tag{5.5.17}$$

when the field is parallel to the magnetization. This relation is only true to first order in $1/J$, and corrections have to be made for the influence of any field-dependent changes of the correlation functions $\sigma$ and $\eta_{\pm}$. Both $A_{\mathbf{q}}(T)$ and $B_{\mathbf{q}}(T)$ may be determined from the energies and initial slopes, since

$$A_{\mathbf{q}}(T) \pm B_{\mathbf{q}}(T) \simeq \tfrac{1}{2}\alpha_{\mathbf{q}}(T) \pm \tfrac{1}{2}[\alpha_{\mathbf{q}}^2(T) - 4E_{\mathbf{q}}^2(T)]^{\frac{1}{2}}. \tag{5.5.18}$$

This method was used by Jensen *et al.* (1975) for a comprehensive study ot the two-ion anisotropy in Tb. The values of $A_{\mathbf{q}}(T)$ and $B_{\mathbf{q}}(T)$, deduced from eqn (5.5.18), were parametrized in various ways, and clearly the best least-squares fit was obtained with expressions of the form

$$\begin{aligned}(A_{\mathbf{q}} + B_{\mathbf{q}}) - (A_{\mathbf{0}} + B_{\mathbf{0}}) &= \mathcal{I}(\mathbf{q}) + \mathcal{K}(\mathbf{q}) - \mathcal{C}(\mathbf{q})\cos 6\phi \\ (A_{\mathbf{q}} - B_{\mathbf{q}}) - (A_{\mathbf{0}} - B_{\mathbf{0}}) &= \mathcal{I}(\mathbf{q}) - \mathcal{K}(\mathbf{q}) - \mathcal{D}(\mathbf{q})\cos 6\phi,\end{aligned} \tag{5.5.19}$$

where $A_{\mathbf{0}} \pm B_{\mathbf{0}}$ were taken from the simultaneous measurements of the magnetic anisotropy at $\mathbf{q} = \mathbf{0}$, discussed in the previous section. The low-temperature isotropic coupling $\mathcal{I}(\mathbf{q})$, which in the absence of anisotropy would just be $J[\mathcal{J}(\mathbf{0}) - \mathcal{J}(\mathbf{q})]$, and the $\phi$-independent two-ion anisotropy $\mathcal{K}(\mathbf{q})$ are shown in Fig. 5.10. The $\phi$-dependent axial

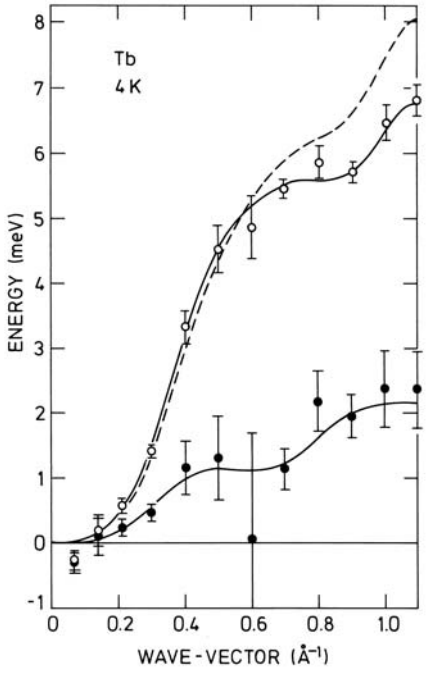


**Fig. 5.10.** Isotropic and anisotropic two-ion coupling parameters $\mathcal{I}(\mathbf{q})$ (upper curve) and $\mathcal{K}(\mathbf{q})$ (lower curve) for Tb at 4 K, deduced from the field dependence of the spin-wave energies. The former is closely related to $J[\mathcal{J}(\mathbf{0}) - \mathcal{J}(\mathbf{q})]$, an estimate of which is indicated by the dashed line. The magnon–phonon interaction causes relatively large uncertainties at intermediate wave-vectors.

anisotropy $\mathcal{C}(\mathbf{q})$ is about the same magnitude as $\mathcal{K}(\mathbf{q})$, while $\mathcal{D}(\mathbf{q})$ is very small. The $\phi$-dependent anisotropy is detected very clearly in the experiments, since it gives rise to a change in the dispersion $E_{\mathbf{q}}(T)$, when the moments are rotated from the the easy to the hard planar direction. $\mathcal{C}(\mathbf{q})$ is the $\mathbf{q}$-dependent generalization of the $\phi$-dependent anisotropy $\Delta M$ in $A_{\mathbf{0}} + B_{\mathbf{0}}$, introduced in the previous section, and $\Delta M \approx -\langle \mathcal{C}(\mathbf{q}) \rangle_{\mathbf{q}}$.

As mentioned in Section 5.4.1, the corrections to the field dependence of the magnon energies in (5.5.17) were included in an effective fashion, neglecting changes due to the rotation of the moments and assuming $\eta_- \simeq 1/\eta_+ \simeq \{1-b(T=0)\}\sigma^{-k}$, where $k$ may be estimated to be about 0.3. The renormalization effects are thus taken as proportional to $\sigma$ raised to a power which depends on the term considered. We estimate that the effects neglected in this approach only introduce corrections of the order of the experimental uncertainties. The two-ion coupling

parameters decrease with increasing temperature or decreasing magnetization. The three anisotropy component all decrease very rapidly, roughly proportionally to $\sigma^{15}$ (like $\Delta M$), which means that they are only important at low temperatures and may be neglected above about 150 K. The strong temperature dependence of the anisotropic components indicates, according to the Callen–Callen theory, that higher-rank couplings make the dominant contribution. The lowest-order term in eqn (5.5.14) which contributes to $\mathcal{C}(\mathbf{q})$ involves $K_{44}^{33}$, and it should renormalize approximately as $\sigma^{19}$. The renormalization is observed to be **q**-dependent for all the parameters, being slower at larger wave-vectors, and it lies in the range $\sigma^2$-$\sigma^{0.1}$ for $\mathcal{I}(\mathbf{q})$. In Tb, $\mathcal{I}(\mathbf{q})$ may include higher-rank contributions besides the RKKY-exchange term, but the way in which it renormalizes resembles quite closely the behaviour observed in Gd and shown in Fig. 5.1. A **q**-dependent renormalization may partially be accounted for, in the self-consistent RPA theory, by the **k**-sum terms in (5.2.38).

When **q** is not along the $c$-axis, there are other ways in which the presence of two-ion anisotropy may be detected in the ferromagnetic excitation spectrum:

(iv) Spin-wave energy gaps may appear at the boundaries of the Brillouin zone.

The isotropic two-ion coupling alone does not lead to energy gaps at these boundaries, whereas anisotropic two-ion couplings may lift those degeneracies which are not dictated by symmetry. In fact, the first indication of the presence of two-ion anisotropy in the rare earth metals, other than the classical magnetic-dipolar interaction, was the splitting shown in Fig. 5.2 along the KH edge of the Brillouin zone in the ferromagnetic phase of Tb (Lindgård and Houmann 1971). Finally, we have the related effect:

(v) The spin-wave energies, at a particular **q**, in domains with different angles between the **q**-vector and the magnetization vectors, need not be equal if two-ion anisotropy is important.

In a single domain, the two-ion anisotropy forces may lift the 'accidental' degeneracies between spin waves at **q**-vectors which are equivalent in the paramagnetic phase, but which are no longer equivalent in the Brillouin zone of the ferromagnet. This manifestation of the two-ion anisotropy has not yet been subjected to experimental investigation, but it may provide a useful supplement to studies of the **q**-dependence of $B_{\mathbf{q}}(T)$.

As we have seen, the expectation values $\langle \widetilde{O}_{lm} \rangle$ are approximately proportional to $\sigma^{l(l+1)/2}$, if the extra modification due to the elliptical polarization of the spin-waves is neglected. This means that the importance of the higher-rank couplings declines relatively rapidly with tem-

perature. The effects of these interactions on the ground state and the spin waves are therefore most pronounced in the low-temperature limit, whereas the behaviour of the system at high temperatures which, in the heavy rare earths, includes the critical region around the phase transition between the ordered and paramagnetic phases, is dominated by the coupling between the dipolar moments, and the single-ion quadrupole interaction, i.e. by the terms in eqn (5.5.14) with $l + l' = 2$.